# Upper limit of metastability of the vortex-free state of a two-dimensional superconductor in a nonuniform magnetic field

Thomas R. Lemberger* and Adam Ahmed†
*Department of Physics, The Ohio State University, Columbus, Ohio, 43210, USA*
(Received 19 April 2013; revised manuscript received 24 May 2013; published 6 June 2013)

We calculate the magnetic field above which vortices necessarily appear in a two-dimensional superconducting film in a nonuniform magnetic field applied near its center, as in two-coil measurements of superfluid density. Experiments suggest that free vortices appear when the Meissner screening current density is large enough that the free-energy barrier for separating tightly-bound vortex-antivortex (V-aV) pairs into free vortices is comparable to $k_B T$, not at the much lower thermodynamic critical field. Specifically, we calculate the applied magnetic field above which there exists no metastable state without vortices. There is a simple analogy with the appearance of phase-slip centers in a one-dimensional superconducting wire.

DOI: 10.1103/PhysRevB.87.214505 PACS number(s): 74.78.−w, 74.25.N−, 74.25.Op, 75.40.Mg

## I. INTRODUCTION

We calculate the applied magnetic field above which vortices necessarily appear in a two-dimensional (2D) superconductor exposed to a nonuniform magnetic field. This field is orders of magnitude larger than the thermodynamic applied field where vortices would appear if not for the high free-energy barrier for breaking nascent vortex-antivortex (V-aV) pairs.[1,2] The calculation is useful for the determination of the in-plane Ginzburg-Landau coherence length $\xi$ from the onset of strong nonlinear effects in two-coil experiments[3–9] measuring the magnetic penetration depth $\lambda$.

Some years ago, Scharnhorst[9] found that vortices appeared in thin quench-condensed films of Sn and In when the induced screening supercurrent due to the magnetic field from a small coil located near the films was near the critical current density. Recent measurements on thin Nb and amorphous MoGe films agree.[10] Since the thermodynamic lower critical field is orders of magnitude smaller than the measured external critical field,[1,2] there must be a high free-energy barrier for creation of vortices. The applied field at which this barrier vanishes has been calculated, e.g., Ref. 11, for films that are at least several coherence lengths thick, which means they are thick enough to sustain vortices lying in the plane of the film. Calculation of the free-energy barrier to unbind V-aV pairs in 2D films, $d < \xi$, is difficult because it involves calculating the free energy of a V-aV pair for center-to-center separations less than $\xi$.

We calculate the highest external magnetic field at which there exists a metastable vortex-free superconducting state. The experimental critical field is necessarily somewhat smaller.[10] There is an instructive analogy to the physics of a 1D superconducting wire.[12] In 1D, there is no stable thermodynamic superconducting state; the zero-resistance state is only metastable because it is interrupted by occasional, short-lived, thermal or quantum phase-slip centers (PSC), which are the 1D analog of bound V-aV pairs.[13,14] If the wire is current-biased by connection to an external current supply, then the zero-resistance state is metastable up to a current where the Cooper-pair momentum $p_s$ reaches $\hbar/\sqrt{3}\xi$. PSC's may occur before that point is reached, but at that point, PSC's necessarily appear regularly. If the wire is a circular loop and the supercurrent within it is established by a magnetic flux passing through the loop's center, then it is effectively voltage-biased. In principle, the PSC-free state can survive up to $p_s = \hbar/\xi$, at which point superconductivity is extinguished throughout the wire. It is likely that PSC's actually appear a bit before that point.

In a 2D superconducting film in a nonuniform field applied near its center, there is a stable vortex-free thermodynamic state only for applied fields below a very small thermodynamic critical field.[1,2] Thus, as a practical matter, the vortex-free state is always metastable just like a 1D wire. We will see that if the superconducting film screens the magnetic field strongly, vortices appear when the peak induced Cooper-pair momentum is $p_s^{\max} = \hbar/\sqrt{3}\xi$; if screening is weak, vortices necessarily appear when $p_s^{\max} = \hbar/\xi$. These results are reminiscent of the current-biased and voltage-biased 1D superconducting wire.

On the experimental side, we are interested in determining $\xi$ from two-coil measurements in the nonlinear regime. This approach appeals because the field in the superconductor at the onset of vortices is typically less than 10 G, and the applied field less than 100 G. Technically, applying 100 G is simpler than applying the tens of teslas that are often necessary to reach the upper critical field, $B_{c2}$. Physically, a 10-G internal field has a much smaller effect on the underlying normal state than tens of teslas and therefore produces a complementary value.

## II. CALCULATION

Our computer program, based on that of Turneaure *et al.*,[5] calculates the diamagnetic sheet supercurrent density $K_s(\rho)$ as a function of radial distance from the center of the film, $\rho$, in a 2D superconducting film exposed to a nonuniform external field. We take into account the suppression of superfluid density associated with the Cooper-pair momentum $p_s(\rho)$. Figure 1 shows the experimental configuration for the two cases explored in this paper: (1) a point-dipole drive coil a distance $h$ below the film, for which $\rho_0 = \sqrt{2}h$, and (2) a loop of radius $R$ located a distance $R$ below the film, for which $\rho_0 = 1.7R$. Here, $\rho_0$ is the radial distance along the film's surface at which the applied perpendicular field changes sign. The program does not include vortices, just the diamagnetic screening supercurrents. When the maximum

 

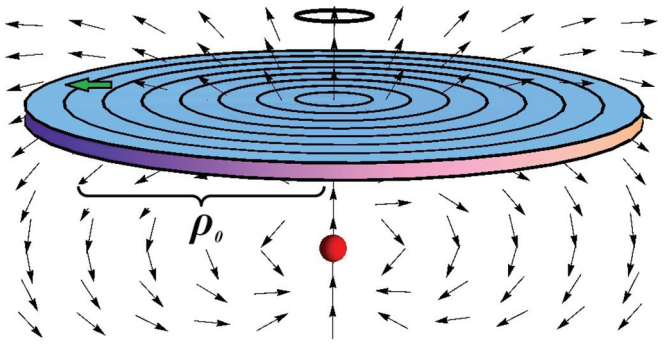


FIG. 1. (Color online) Setup modeled in the MATLAB program. The external magnetic field is produced by the red sphere below the film, which represents one of two cases: a point-dipole drive coil or a loop of radius $R$. The pick-up coil is represented by the single-turn loop above the film. The film is represented as a collection of concentric rings, which is how it is modeled numerically. The drive coil, pick-up coil, and film are coaxial, and the film is midway between drive and pick-up coils. Arrows represent the magnetic field from the drive coil at an instant in time. The green arrow pointing to the left shows where the applied field is parallel to the film, i.e., the perpendicular component vanishes. The radius at which this occurs is defined as $\rho_0$. The setup is not drawn to scale.

applied perpendicular field exceeds a certain threshold, the program fails to converge, indicating that there is no metastable nonvortex state at that applied field.

There are two regimes to consider: strong and weak screening, defined by the relationship between the microscopic scale, $\Lambda$, and the experimental length scale, $\rho_0$. $\Lambda$ is the 2D penetration depth,[15] $\Lambda \equiv 2\lambda^2/d$, ($\lambda$ is the bulk penetration depth). The strong screening regime is $\rho_0 >> \Lambda$, wherein the magnetic field above the film is much smaller than the field applied below the film. In the weak-screening regime, $\rho_0 << \Lambda$, the field above the film is only slightly smaller than the applied field.

The strategy of the numerical calculation is the following. First, we calculate the linear-response sheet supercurrent density, $K_s(\rho)$, and Cooper-pair momentum, $p_s(\rho)$, for a given applied field at the center of the film, $B_0$, with the assumption of a uniform superfluid density, $n_s(\rho) = n_{s0}$, i.e., for a particular value of $\rho_0/\Lambda \propto n_{s0}$. Second, we adjust $n_s(\rho)$ according to[12] $n_s(\rho)/n_{s0} = 1 - p_s^2(\rho)\xi^2/\hbar^2$. Then we recalculate $K_s(\rho)$ and $p_s(\rho)$ with the adjusted $n_s(\rho)$. This process is repeated until it converges. Then we increase $B_0$ and repeat the calculation. For a given $\rho_0/\Lambda$, eventually $B_0$ reaches a value above which

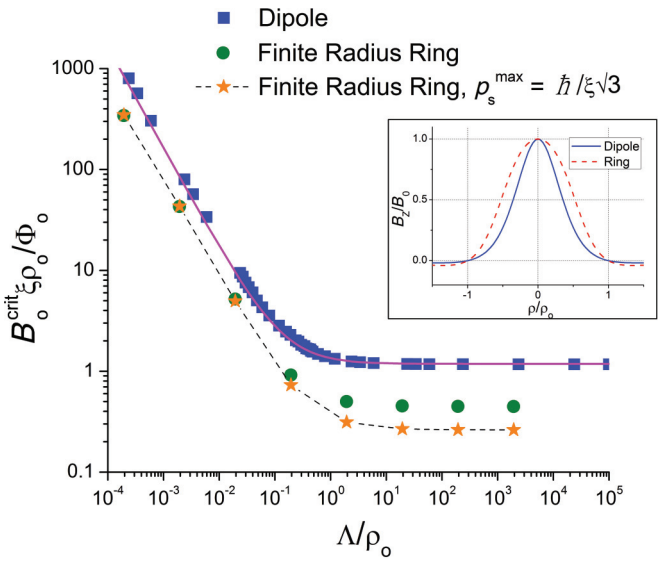


FIG. 2. (Color online) $B_0^{\rm crit}\xi\rho_0/\Phi_0$ vs $\Lambda/\rho_0$ for a point dipole drive coil (uppermost square points), a single-turn drive coil of radius $R$ located a distance $R$ below the film (middle round points), and the critical field calculated assuming that vortices appear when the peak Cooper-pair momentum $p_s^{\rm max}$ reaches $\hbar/\sqrt{3}\xi$, (bottom star points). The solid curve is $B_0^{\rm crit}\xi\rho_0/\Phi_0 = (3\sqrt{6} + \rho_0/\Lambda)/2\pi$, and it fits the point-dipole drive coil calculation well. (Inset) Applied perpendicular magnetic field for point-dipole and single-turn drive coils.

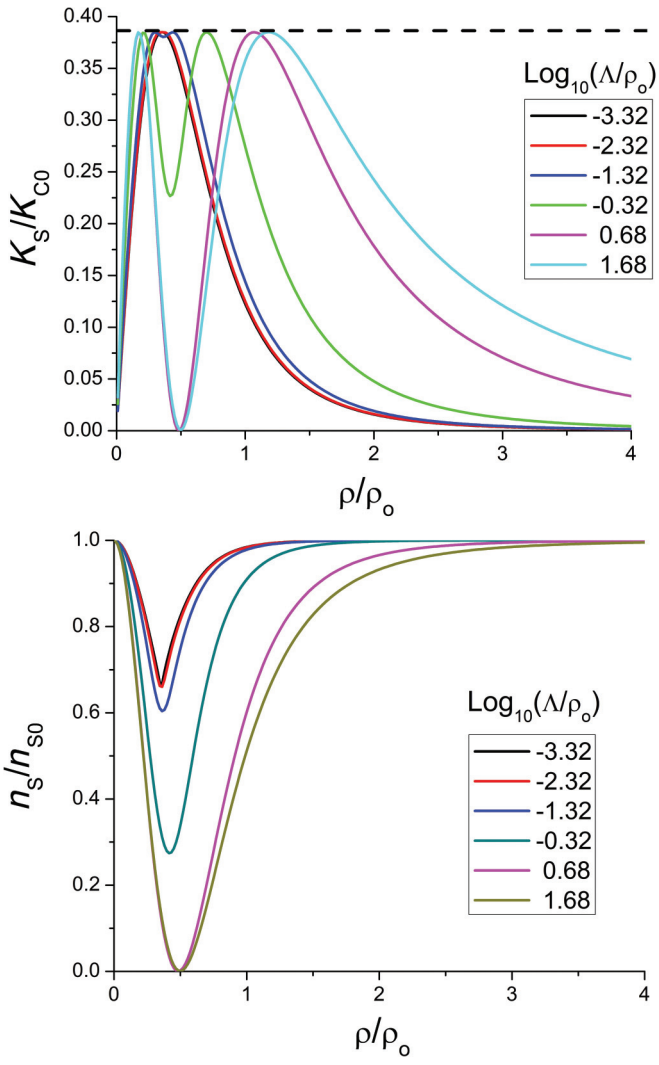


FIG. 3. (Color online) Normalized (top) screening sheet supercurrent density $K_s/K_{c0}$ and (bottom) superfluid density $n_s/n_{s0}$ vs $\rho/\rho_0$ at $B_0 = B_0^{\rm crit}$, for different $\Lambda/\rho_0$, for a point-dipole drive coil. $K_{c0} \equiv dn_{s0}e\hbar/2m\xi = \Phi_0/\pi\Lambda\xi$, where $n_{s0}$ is the unperturbed density of superconducting electrons, and $2m$ is the mass of a Cooper pair. (Top) The horizontal dotted line represents the Ginzburg-Landau critical sheet current density ($2K_{c0}/3\sqrt{3}$) and is shown as an upper bound on $K_s$ for all levels of screening. (Bottom) The dip in $n_s/n_{s0}$ reaches zero at $\Lambda/\rho_0 = 1/2$.

the program no longer converges. We define this critical field as $B_0^{\rm crit}(\rho_0/\Lambda)$. We also record the value of $B_0$ at which the peak superfluid momentum $p_s^{\rm max}$ in the film reaches $\hbar/\sqrt{3}\xi$, because this field may be closer to the experimentally observed critical field.

### III. RESULTS

Figure 2 shows the main result of this paper: the relationship between $B_0^{\rm crit}$ and $\xi$ for different values of the "screening parameter" $\Lambda/\rho_0$. The weak-screening regime is most likely to be encountered for $T$ near $T_c$, where $\Lambda$ diverges. For a point-dipole drive coil, a good fit is provided by $B_0^{\rm crit}\xi\rho_0/\Phi_0 = (3\sqrt{6}+\rho_0/\Lambda)/2\pi$. The constant term, $3\sqrt{6}/2\pi$, can be obtained analytically in the weak-screening regime where the vector potential inside the film is essentially equal to the applied vector potential. The other term, $\rho_0/2\pi\Lambda$, is empirical. For the single-turn drive coil, the calculated $B_0^{\rm crit}$ is smaller by a factor of about 2.5 in the weak-screening regime. The lowest curve is calculated assuming that vortices appear when the peak Cooper-pair momentum, $p_s^{\rm max}$, reaches $\hbar/\sqrt{3}\xi$. The inset shows the perpendicular applied field for both drive coils.

Figures 3 and 4 show normalized sheet supercurrent density, $K_s(\rho/\rho_0)$, superfluid density, $n_s(\rho/\rho_0)$, and Cooper pair momentum, $p_s(\rho/\rho_0)$, at $B_0 = B_0^{\rm crit}$ for several values of $\Lambda/\rho_0$, for a point-dipole drive coil. From Fig. 4, we see that when $\Lambda/\rho_0 << 1$, application of the critical field results in a peak superfluid momentum, $p_s^{\rm max}$, that is slightly larger than $\hbar/\sqrt{3}\xi$. Thus $n_s(\rho)$ has a minimum (see Fig. 3), but is nonzero everywhere. At $\Lambda/\rho_0 = 1/2$, the peak Cooper-pair momentum at the critical field reaches $\hbar/\xi$, so $n_s = 0$ on a circle. For $\Lambda/\rho_0 > 1/2$, we define the critical applied field to be the field where $n_s$ is first suppressed to zero along a circle. This is important to say because in this regime the program converges for any applied field $B_0$. At fields higher than $B_0^{\rm crit}$, the program converges to states where $n_s = 0$ over a circular band of nonzero width, rather than on a circular line.

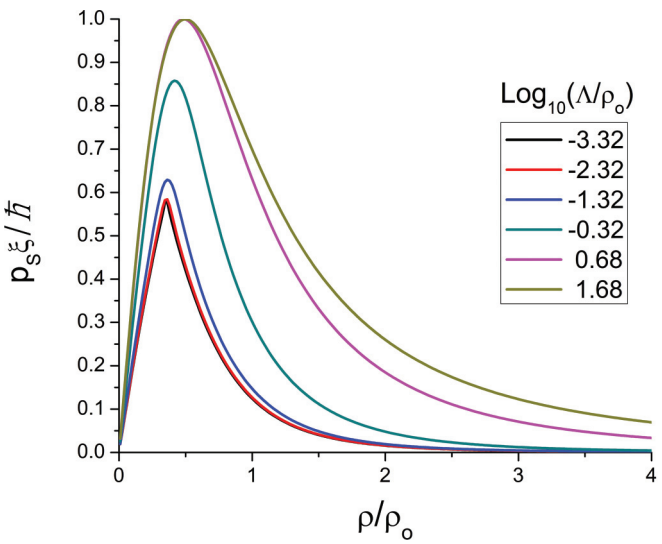


FIG. 4. (Color online) Normalized Cooper pair momentum $p_s\xi/\hbar$ vs $\rho/\rho_0$. For $\Lambda << \rho_0$, $p_s\xi/\hbar$ has a peak value slightly greater than $1/\sqrt{3}$. For $\Lambda > \rho_0/2$, the peak is at unity.

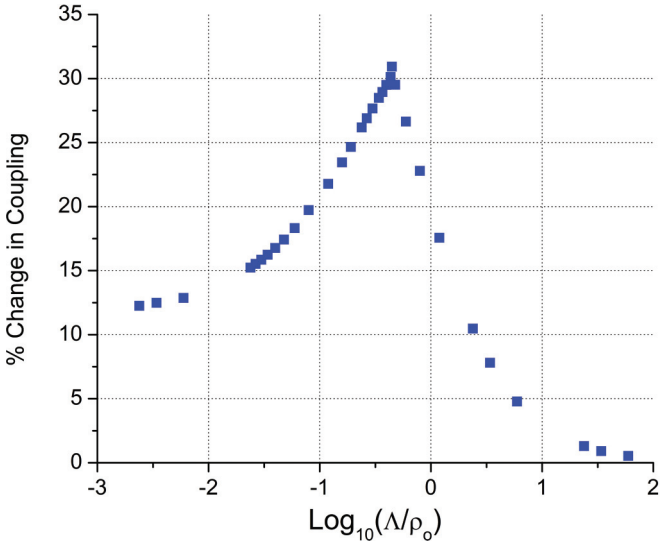


FIG. 5. (Color online) Flux in the pick-up coil, normalized to its linear-response value, when the applied field from a point-dipole drive coil increases from $B_0 = 0$ to $B_0 = B_0^{\rm crit}$. Practically speaking, at liquid He temperatures, we expect most superconducting films to lie within $\mathrm{Log}_{10}(\Lambda/R) \in [-3,0]$. Thus we expect a 10% to 30% change in coupling before strong nonlinear effects appear.

Figure 5 shows the flux in the pick-up coil at an applied field of $B_0^{\rm crit}$ as a function of screening, $\mathrm{Log}_{10}(\Lambda/\rho_0)$, for a point-dipole drive coil. The pick-up flux is normalized to its linear-response value. The discontinuity in slope at $\Lambda/\rho_0 = 1/2$ occurs because, as mentioned above, for $\Lambda/\rho_0 \geqslant 1/2$, the first vortex-bearing state has $n_s = 0$ along a circle, whereas for $\Lambda/\rho_0 < 1/2$, vortices appear before $n_s$ is suppressed to zero anywhere.

Another way to view the nonlinear behavior that precedes the appearance of vortices is to consider the flux in the

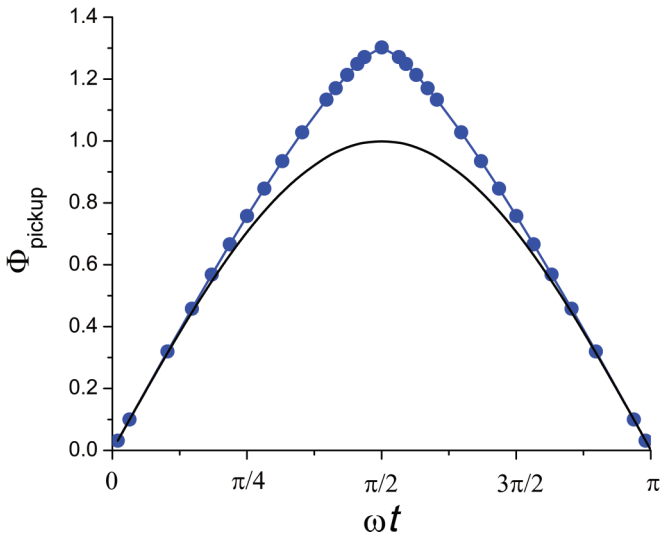


FIG. 6. (Color online) Magnetic flux in the pick-up coil vs dimensionless time, $\omega t$, for $\Lambda/\rho_0 = 0.35$. The peak applied field from a point-dipole drive coil is $B_0^{\rm crit}$ at $\omega t = \pi/2$. The lower curve is linear response. The upper curve (through circular calculated points) is the calculated nonlinear response.

pick-up coil as a function of time for a sinusoidal applied field. Figure 6 shows the magnetic flux linked to the pick-up coil for one-half cycle for the case $\Lambda/\rho_0 = 0.35$. The lower sinusoidal curve represents linear response; the upper triangular curve illustrates the nonlinear response from our calculations. The peak applied field is $B_0^{\rm crit}$, where the pickup flux is 30% higher than for linear response. A lock-in amplifier measuring the flux pickup at the fundamental frequency would detect a signal about 7% higher than for linear response.

## IV. CONCLUSION

We have calculated the external magnetic field above which vortices must appear in a two-dimensional superconducting film exposed to the nonuniform magnetic field of a point dipole or from a single-turn drive coil. For a point-dipole, we find $B_0^{\rm crit}\xi\rho_0/\Phi_0 \approx (3\sqrt{6} + \rho_0/\Lambda)/2\pi$, where $B_0$ is the dipole's field at the center of the film. For typical solenoidal coils, $B_0^{\rm crit}\xi\rho_0/\Phi_0$ is about 2.5× smaller in the weak-screening regime. In principle, a low-field measurement of $\Lambda(T)$ and a "high-field" measurement of $B_0^{\rm crit}(T)$ together suffice to determine the coherence length $\xi(T)$. In practice, "high-field" means ten gauss or less, as opposed to the tens of teslas often needed to determine $\xi$ from measurements of the upper critical field, $B_{c2}$.

## ACKNOWLEDGMENTS

We acknowledge useful discussions with John Draskovic. This work was supported in part by DOE-Basic Energy Sciences through Grant No. FG02-08ER46533.

*trl@physics.osu.edu
†ahmed.274@osu.edu

[1] T. R. Lemberger and J. Draskovic, Phys. Rev. B **87**, 064503 (2013).
[2] A. L. Fetter and P. C. Hohenberg, Phys. Rev. **159**, 330 (1967).
[3] A. F. Hebard and A. T. Fiory, Phys. Rev. Lett. **44**, 291 (1980).
[4] A. T. Fiory and A. F. Hebard, Appl. Phys. Lett. **52**, 2165 (1988).
[5] S. J. Turneaure, E. R. Ulm, and T. R. Lemberger, J. Appl. Phys. **79**, 4221 (1996).
[6] S. J. Turneaure, A. A. Pesetski, and T. R. Lemberger, J. Appl. Phys. **83**, 4334 (1998).
[7] J. H. Claassen, M. E. Reeves, and R. J. Soulen, Rev. Sci. Instrum. **62**, 996 (1990).
[8] J. H. Claassen and R. H. Ono, Appl. Phys. Lett. **74**, 4023 (1999).
[9] P. Scharnhorst, Phys. Rev. B **1**, 4295 (1970).
[10] J. Draskovic, T. R. Lemberger, B. Peters, F. Y. Yang, S. Wang, J. Ku, and A. Bezryadin (unpublished).
[11] Y. Mawatari and J. R. Clem, Phys. Rev. B **74**, 144523 (2006).
[12] M. Tinkham, *Introduction to Superconductivity*, 2nd ed. (Dover, New York, 2004).
[13] W. J. Skocpol, M. R. Beasley, and M. Tinkham, J. Low Temp. Phys. **16**, 145 (1974).
[14] J. S. Langer and V. Ambegaokar, Phys. Rev. **164**, 498 (1967).
[15] J. Pearl, Appl. Phys. Lett. **5**, 65 (1964).